Solar Phys (2011) 269: 309–333
DOI 10.1007/s11207-011-9710-0

Particle Acceleration and Propagation in Strong Flares without Major Solar Energetic Particle Events

K.-L. Klein · G. Trottet · S. Samwel · O. Malandraki

Received: 20 October 2010 / Accepted: 5 January 2011 / Published online: 10 February 2011

Abstract Solar energetic particles (SEPs) detected in space are statistically associated with flares and coronal mass ejections (CMEs). But it is not clear how these processes actually contribute to the acceleration and transport of the particles. The present work addresses the question why flares accompanied by intense soft X-ray bursts may not produce SEPs detected by observations with the GOES spacecraft. We consider all X-class X-ray bursts between 1996 and 2006 from the western solar hemisphere. 21 out of 69 have no signature in GOES proton intensities above 10 MeV, despite being significant accelerators of electrons, as shown by their radio emission at cm wavelengths. The majority (11/20) has no type III radio bursts from electron beams escaping towards interplanetary space during the impulsive flare phase. Together with other radio properties, this indicates that the electrons accelerated during the impulsive flare phase remain confined in the low corona. This occurs in flares with and without a CME. Although GOES saw no protons above 10 MeV at geosynchronous orbit, energetic particles were detected in some (4/11) confined events at Lagrangian point L1 aboard ACE or SoHO. These events have, besides the confined microwave emission, dm-m wave type II and type IV bursts indicating an independent accelerator in the corona. Three of them are accompanied by CMEs. We conclude that the principal reason why major solar flares in the western hemisphere are not associated with SEPs is the confinement of particles accelerated in the impulsive phase. A coronal shock wave or the restructuring of

K.-L. Klein (✉) · G. Trottet
Observatoire de Paris, LESIA-CNRS UMR 8109, Univ. P & M Curie and Paris-Diderot, Observatoire de Meudon, 92195 Meudon, France
e-mail: ludwig.klein@obspm.fr

G. Trottet
e-mail: gerard.trottet@obspm.fr

S. Samwel
National Research Institute of Astronomy and Geophysics (NRIAG), Helwan, Cairo, Egypt
e-mail: samwelsw@nriag.sci.eg

O. Malandraki
Institute of Astronomy and Astrophysics, National Observatory of Athens, 11810 Athens, Greece
e-mail: omaland@astro.noa.gr

the magnetically stressed corona, indicated by the type II and IV bursts, can explain the detection of SEPs when flare-accelerated particles do not reach open magnetic field lines. But the mere presence of these radio signatures, especially of a metric type II burst, is not a sufficient condition for a major SEP event.

Keywords Corona, radio emission · Energetic particles, acceleration · Energetic particles, propagation · Flares, energetic particles · Flares, relation to magnetic field

1. Introduction

The role of flares and coronal mass ejections (CMEs) in the acceleration and propagation of solar energetic particles (SEPs) detected in space is a subject of ongoing debate. SEP events, as routinely monitored with the *Geosynchronous Operational Environmental Satellites* (GOES) operated by NOAA, are statistically associated with both flares and fast and broad CMEs (Cane, Erickson, and Prestage, 2002; Gopalswamy *et al.*, 2004). More detailed statistical analyses that attempted to correlate SEP parameters with those of the associated flares and CMEs did not establish an unambiguous conclusion so far. In this situation it appears useful to investigate events where the association is less ambiguous than usual.

Previous studies showed that CMEs without radio signatures of electron acceleration in the corona (Marqué, Posner, and Klein, 2006) and strong flares without CMEs (Klein, Trottet, and Klassen, 2010) are not accompanied by major SEP events, the term "major" meaning SEP events detected by patrol observations with the GOES spacecraft. Here we address the more general question under which conditions large solar flares do not produce SEP events. We select large flares by their peak soft X-ray emission in order to have a prominent identifier of solar activity and thereby to minimise any chance coincidence. As a handy criterion we use the peak soft X-ray flux and limit ourselves to X-class events, where the peak soft X-ray flux in the 0.1 – 0.8 nm band is 10^{-4} W m^{-2} or higher. There need not be a direct physical relationship between soft X-ray peak intensity, which is a parameter referring to the thermal plasma, and the non thermal particle intensity in space. But in the sense of Kahler's "big flare syndrome" (Kahler, 1982b) there is a rough expectation that flare/CME events with a prominent manifestation in one spectral domain have a better chance to have prominent signatures in other domains, too. Therefore the restriction to X-class flares is a practical starting point. Indeed Belov *et al.* (2007) showed that the association of SEP events increases with increasing importance of the soft X-ray burst, but that 30 – 40% of bursts of class X lack an SEP event. They are the target of the present study.

In order to identify potential accelerators and conditions for charged particle propagation in the corona, we employ radio emissions from cm to km wavelengths, emitted by non thermal electrons between the low corona and the Earth. The present paper is organised as follows: in Section 2 the list of flares with X-class soft X-ray emission is established, and SEP signatures are searched for in the particle data of the GOES spacecraft. 21 X-class flares without SEP detection are identified. Details are given in Appendix A. The association of these events with radio emission and CMEs is analysed in Section 3 (details in Appendix B), and electron and proton signatures are searched for in measurements near the L1 Lagrangian point. Results are discussed in Section 4 with respect to the confinement of particles accelerated during the impulsive phase and the role of acceleration in coronal shock waves and during the restructuring of the magnetically stressed corona in the course of a CME. A summary is given in Section 5.

2. Strong Soft X-Ray Bursts and SEP Events

Starting with the list of GOES soft X-ray bursts between 1996 and December 2006 compiled by NOAA[1] we identified all X-class bursts located between longitudes W0° and W90°. The detailed procedure, references and the event list are described in Appendix A. The flare location was identified through the associated Hα signature in the event list or in the Comprehensive Reports of *Solar Geophysical Data* (henceforth abbreviated SGD), or using the location of an EUV brightening observed by the Extreme Ultraviolet Telescope (EIT) aboard the *Solar and Heliospheric Observatory* (SoHO; Delaboudinière *et al.*, 1995). A total of 69 X-class flares were observed in the western solar hemisphere.

We then searched for SEP events in the observations by the GOES Space Environment Monitor's Energetic Particle Sensor (EPS) at proton energies above 10 MeV. The majority of the flares was followed by a GOES SEP event, although only 21 are contained in the SEP event list maintained at NOAA.[2] Many events are eliminated by the threshold criteria applied by NOAA for the event identification.

21 GOES X-class flares (30% of the sample) in the western solar hemisphere were found to have no SEPs in excess above the background of GOES/EPS. In the following we shall use the term "SEP-less" for these flares. The fraction of SEP-less flares agrees with the one reported by Belov *et al.* (2007) who used slightly different criteria (a longitude range from E20° to W90°) and a larger event sample. The intensities of the SEP-less X-class flares in our sample range from X1.1 to X2.7. Flares of class X3 and higher in the western hemisphere did produce SEP events detected at GOES. Belov *et al.* (2007) found that all soft X-ray bursts in classes above X6.2 west of E20° were accompanied by SEP events.

3. Radio Emission and CME Association of SEP-Less X-Class Flares

Why does a strong flare in the western hemisphere of the Sun not produce SEPs detected at geosynchronous orbit by the GOES monitors? Possible reasons include the limited sensitivity of the GOES detector, conditions of acceleration at and escape from the Sun, or else a poor magnetic connection of the flaring active region to the Earth, despite the fact that our restriction to flares in the western hemisphere should reduce this problem.

3.1. Sensitivity of the GOES Particle Detector – Comparison with SoHO/ERNE

The fact that all X-ray bursts in the western hemisphere with peak flux $\geq 3 \times 10^{-4}$ W m^{-2} are accompanied by GOES SEP events suggests that sensitivity plays a role. To further investigate this, we examined the deka-MeV proton measurements of the Energetic and Relativistic Nuclei and Electron Experiment (ERNE) aboard SoHO (Torsti *et al.*, 1995).[3] The ERNE HED detector has an energy-dependent geometric factor decreasing from about 40 cm^2 sr at 10 MeV to 25 cm^2 sr near 100 MeV (see Figure 3 of Torsti *et al.*, 1995), which is two orders of magnitude above that of the GOES/EPS "Dome" device (*GOES Data Book*[4]). ERNE detected significant proton events in four of the 21 cases with no SEP

[1] http://www.ngdc.noaa.gov/stp/SOLAR/.

[2] http://www.swpc.noaa.gov/ftpdir/indices/SPE.txt.

[3] Data provided through http://www.srl.utu.fi/erne_data/datafinder/df.shtml.

[4] http://goes.gsfc.nasa.gov/text/goes.databook.html.

signature at GOES. Ten events had no signature in ERNE data. In the remaining seven cases the background from previous events was high and might mask minor new particle injections. In any case, since in most events the upper intensity limit from the GOES SEP measurements is significantly lower than the value expected from the soft X-ray properties after Garcia (2004), other explanations must be searched for.

3.2. Radio Emissions as Tracers of Electron Acceleration, Confinement, and Escape

A prime indicator of particle acceleration in the parent flare is the radio emission at cm wavelengths (microwaves). It is emitted by mildly relativistic electrons through gyro-synchrotron radiation in the low corona, where magnetic field strengths are a few hundreds of gauss. The access of energetic electrons to higher coronal layers can be traced by emissions at longer wavelengths: since the thermal electron density and hence the electron plasma frequency decreases with increasing altitude in the corona, emission at dm-m wavelengths comes from higher altitudes than the microwave emission. The emissions at these wavelengths are mostly coherent, and are produced by electron beams (type III bursts), electron populations accelerated at travelling shocks (type II bursts) and during magnetic reconnection in the aftermath of a CME, which generate broadband emissions lasting 10 min to several hours (type IV bursts). Such broadband emissions can also be generated through gyrosynchrotron radiation of mildly relativistic electrons. We employ these types of radio emission by electrons as a tracer of the acceleration and propagation of energetic particles in general. The reader is referred to the reviews of Bastian, Benz, and Gary (1998), Nindos *et al.* (2008) and Pick and Vilmer (2008) for more detailed accounts of the radiation processes.

Five of the 21 X-class flares without SEPs as seen by GOES had no CME. They were discussed in Klein, Trottet, and Klassen (2010). It was shown in that paper, and previously in Gopalswamy, Akiyama, and Yashiro (2009) and Klein, Trottet, and Vilmer (2009), that the flares were efficient electron accelerators, as indicated by conspicuous microwave bursts. But the events had no simultaneous type III bursts at decametric – hectometric waves (abbreviated DH type III bursts in the following). Since DH type III bursts are emitted by subrelativistic electron beams escaping along open magnetic flux tubes through the high corona ($\gtrsim 2R_\odot$ above the photosphere), their non-detection suggests that no electrons actually escaped towards interplanetary space during these events. Further indicators that the microwave-emitting electrons remained confined in low coronal magnetic structures are (Klein, Trottet, and Klassen, 2010): *i*) a steeply rising low-frequency microwave spectrum, which indicates emission from a dense plasma, hence from low coronal heights, and *ii*) the absence of simultaneous emission at dm-m-wavelengths.

Using spectrographic radio observations at decametre and longer wavelengths by the WAVES instrument aboard the *Wind* spacecraft (Bougeret *et al.*, 1995), we were able to characterise 11/21 SEP-less events as "confined microwave events", where no DH type III burst was observed during the impulsive flare phase, *i.e.* between the start and maximum of the soft X-ray burst. Note that this term is different from the common use of "confined flare" as synonymous with "CME-less flare". 9/21 events were non-confined, one event could not be classified, because no WAVES data were available. The criterion for confinement we apply here does not include the prolonged "gradual" or "extended" phase of particle acceleration evidenced by prolonged microwave emission after the soft X-ray maximum (*cf.* Trottet, 1986; Cliver *et al.*, 1986; Kocharov *et al.*, 1994; Bruggmann *et al.*, 1994; Akimov *et al.*, 1996). In the radio range, these events are usually associated with bursts of type II and type IV (see also Pick, 1986). Since these acceleration processes operate at different places from the impulsive acceleration, we will consider type II and type IV radio bursts separately.

As an additional check of the escape of electrons from the corona we analysed the measurements of electrons at deka-to-hecto-keV energies by the Electron, Proton, and Alpha Monitor (EPAM) aboard the *Advanced Composition Explorer* (ACE; Gold *et al.*, 1998) near the Lagrangian point L1. Only the deflected electron channels were used.

3.3. Magnetic Connection

Although our initial selection was restricted to flares in the western hemisphere, flare-accelerated particles can still go undetected by GOES just because the acceleration region is not magnetically connected to the Earth. This is especially the case since we applied no restriction on the latitude of the flare. We roughly estimate the quality of the magnetic connection for each event, evaluating the distance in longitude and latitude between the reported flare position and the footpoint of the nominal Parker spiral. We assume that the Earth-connected Parker spiral is rooted at the apparent latitude of the solar equator as seen from Earth, B_0, and longitude W57°, regardless of the actual solar wind speed. The criterion is very rough, because flare-accelerated particles can be transported over tens of heliocentric degrees in longitude and latitude along diverging open magnetic flux tubes in the corona (Klein *et al.*, 2008), because the time-varying interplanetary magnetic field broadens the range of possible connections (Ippolito *et al.*, 2005), and finally because deviations from constant solar wind expansion speed and the radius of the actual source surface introduce further uncertainty (Nolte and Roelof, 1973).

3.4. Results

A detailed account of the observations is given in Appendix B. From this analysis we derived a rough characterisation of the X-class flares without GOES SEPs in terms of localisation, radio properties and CME association, given separately for confined and non-confined microwave events in Tables 1 and 2, respectively. The entries in the tables are the following:

- The heading 'SEP at L1' indicates if a proton event was observed or not (entry N) by SoHO/ERNE or an electron event by ACE/EPAM. From visual inspection of the intensity time histories we characterise the events as "clean" (C) when the intensity shows a clear rise corresponding in time with the flare, or "marginal" (M) when the signature is weak or appears just as the flattening of the decay of a previous event. See Figure 5 of Klein, Trottet, and Klassen (2010) for an illustration of the marginal 9 June 2003 event. Questionable cases, especially those where a preceding event created a strong and variable background on top of which a new release is difficult to identify, are indicated by a question mark, data gaps by a hyphen. The clean events on 23 November 1998, 11 June 2003, 13 and 18 August 2004 have peak electron intensities of about 10^3 to several 10^3 $(\mathrm{MeV\,cm^2\,sr\,s})^{-1}$ in the 38 – 53 keV range, while the events on 29 May 2003 and 30 October 2004 attain several 10^4 to 10^5 $(\mathrm{MeV\,cm^2\,sr\,s})^{-1}$. For comparison, the major events studied by Haggerty and Roelof (2002, their Figure 3) range from 10^3 to 10^6 electrons $(\mathrm{cm^2\,sr\,s\,MeV})^{-1}$. The 9 July 1996 event occurred before the launch of ACE, but the entry has to be 'C' because energetic electrons were clearly observed in space by Ulysses/HISCALE (Pick *et al.*, 1998) and SoHO/COSTEP (Laitinen *et al.*, 2000). It was also a clear proton event on a very low solar minimum background, with a peak proton intensity in the 12 – 20 MeV range, slightly below 2×10^{-3} $(\mathrm{cm^2\ s\ sr\ MeV})^{-1}$ (see Figure 2 of Laitinen *et al.* (2000)). If we assume a power-law energy spectrum with index 4, this implies an integral intensity

Table 1 Properties of GOES SEP-less X-class flares: confined microwave events.

	1996 07 09	1999 11 27	2000 03 24	2001 04 02	2001 11 25	2002 07 03	2002 10 31	2003 06 09	2004 02 26	2004 08 13	2004 08 18
SEP at L1											
ERNE protons	C	N	–	N	?	N	N	?	N	C	C
EPAM electrons	(C)	N	N	N	N	N	N	M	N	C	C
Magnetic connection											
Longitude	M	W	M	W	–	W	P	–	P	P	P
Latitude	W	M	M	M	–	M	M	–	M	M	M
Microwave burst											
Peak frequency	L	H	H	H	H	H	L	H	L	L	H
Peak flux density	H	L	H	M	L	M	H	M	L	L	M
LF spectral slope	F	F	F	–	–	S	S	M	S	S	S
DH type III											
DH III	Y	N	Y	N	Y	Y	Y	Y	N	Y	Y
during impulsive phase	N	N	N	N	N	N	N?	N	N	N	N
at microwave peak	N	N	N	N	N	N	N	N	N	N	N
II, IV – DH III											
m-λ type II	Y	N	Y	N	N	N	N	Y	N	N	Y
DH III with m-λ II	Y	N	Y	N	N	N	N	Y	N	N	Y
m-λ type IV	Y	N	Y?	N	N	N	N	N	N	Y	Y
DH III with m-λ IV	Y	N	?	N	N	N	N	N	N	Y	Y
CME/dimming	Y	?	–	N	N	Y	N	N	N	Y	Y
CME speed	M	–	–	–	–	S	–	–	–	M	M

above 10 MeV of 3.5×10^{-2} pfu, which is consistent with the upper limit of 0.19 pfu inferred from GOES observations (Table 3).[5]

- The magnetic connection of the flare to the Earth is characterised in the two following lines. The flare is labelled 'well connected' (entry W) if it occurred within $\pm 15°$ of the nominal connection, while the connection is called 'moderate' (M) for distances in the range $\pm (15° - 30°)$ and 'poor' (P) for larger distances.
- The microwave burst spectrum at the time of maximum emission is characterised by the peak frequency, the peak flux density and the low-frequency spectral slope. Peak frequency is high (H) when above 10 GHz, low (L) otherwise. 10 GHz is often quoted as the typical peak of solar microwave bursts. The peak flux density is considered high (H) when ≥ 2000 sfu, moderate (M) between 800 and 2000 sfu, low (L) for flux densities below 800 sfu. There is no objective criterion for these numerical values, they have been selected such as to divide the 20 flares in three groups with about equal numbers of events. The low-frequency spectrum is called steep (S) when the power law spectral index $\alpha_{\rm lf}$ was above 2.5 (flux density $\sim$ frequency$^{\alpha_{\rm lf}}$), moderate (M) when $2.0 \leq \alpha_{\rm lf} \leq 2.5$, and flat (F) when $\alpha_{\rm lf} < 2$. $\alpha_{\rm lf} = 2.5$ is expected for self-absorbed synchrotron emission of relativistic

[5] 1 pfu (particle flux unit) = 1 cm^{-2} s^{-1} sr^{-1}.

Table 2 Properties of GOES SEP-less X-class flares: non-confined microwave events.

	1998 11 23	1999 08 02	1999 08 28	2000 11 24	2002 07 18	2002 08 21	2003 05 29	2003 06 11	2004 10 30
SEP at L1									
ERNE protons	N	N	C	?	N	N	?	N	?
EPAM electrons	C	?	M	N	M	N	C	C	C
Magnetic connection									
Longitude	P	W	P	P	M	W	M	W	P
Latitude	P	M	P	M	W	M	W	W	W
Microwave burst									
Peak frequency	L	H	L	L	H	H	L	L	H
Peak flux density	L	M	H	L	M	M	H	L	H
LF spectral slope	F	F	F	F	F	M	F	M	F
DH type III									
DH III	Y	Y	Y	Y	Y	Y	Y	Y	Y
during impulsive phase	Y	Y	Y	Y	Y	Y	Y	Y	Y
at microwave peak	N	Y	Y	Y	Y	Y	Y	Y	Y
II, IV – DH III									
m-λ type II	N	Y	Y	Y	Y	Y	Y?	Y	Y
DH III with m-λ II	N	Y	Y	Y	Y	N	?	N	Y?
m-λ type IV	Y?	?	N	N	Y	N	Y	N	Y
DH III with m-λ IV	?	?	N	N	Y	N	Y	N	Y
CME/dimming	–	Y	Y	Y	Y	Y	Y	Y	Y
CME speed	–	S	M	F	F	S	F	–	M

electrons, but most often much flatter spectra are observed (Nita, Gary, and Lee, 2004), probably due to the magnetic field variation across the source.

- The existence and timing of DH type III bursts and metric type II and type IV bursts are indicated in the following lines. Type IV bursts may have a smooth spectrum that does not stand out in a dynamic spectrogram and is more easily missed in a routine analysis than a type II burst. So the entries about type IV bursts are probably to be considered with more caution than those on type II bursts.
- The last two lines of the tables indicate whether a CME was associated with the event or not, and give a speed estimate. The association with a CME is considered to be given if the flare is in the vicinity of the CME as seen by the Large Angle and Spectrometric COronagraph (LASCO) aboard SoHO (Brueckner *et al.*, 1995), and if the height – time diagram of the CME front extrapolates backwards to the solar limb and the disk centre near the time of the flare, or if a localised EUV dimming occurred during the flare in the same active region. The CMEs with LASCO observations are indicated as "slow" (S; < 400 km s^{-1}), "fast" (F; > 800 km s^{-1}) or "moderate" (M).

3.5. Illustrative Examples

In this section we present some illustrative examples. Figure 1 displays the soft X-ray (top) and radio observations during a confined microwave event. The dynamic spectrum in the

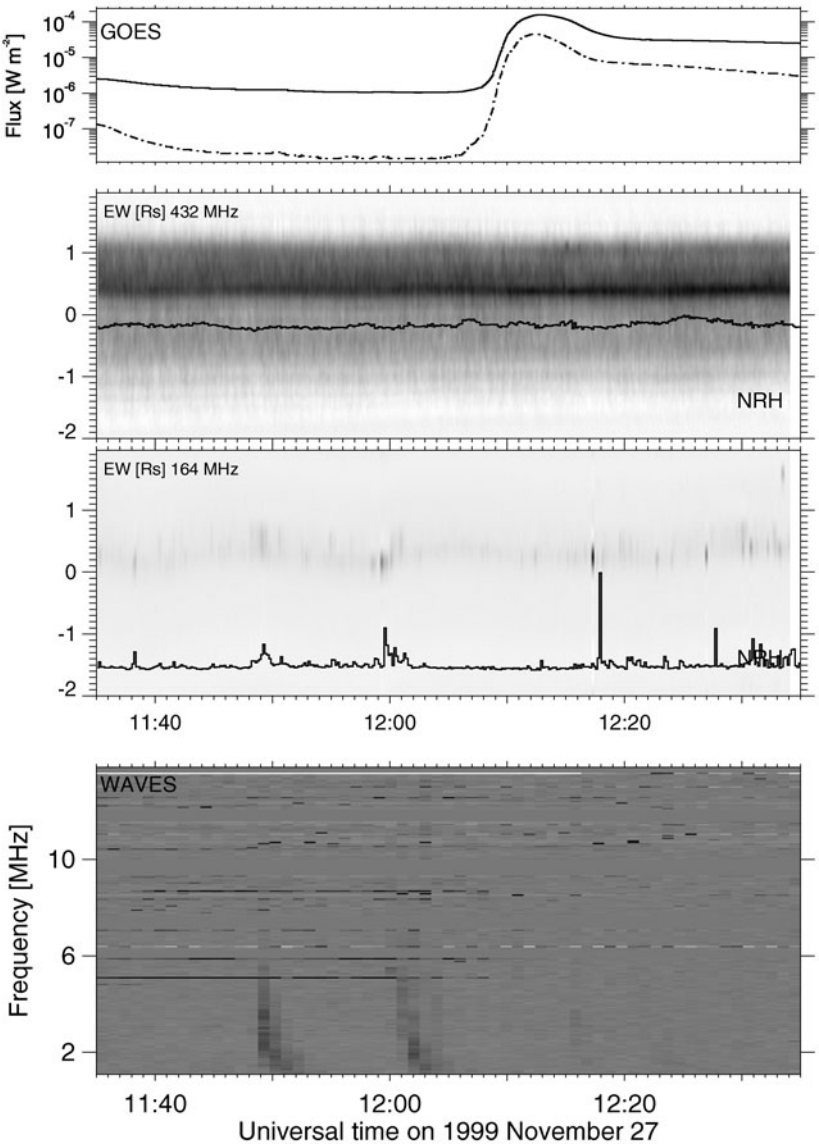

Figure 1 Time histories of X-ray and radio emissions on 27 November 1999. From top to bottom: (1) soft X-ray flux (GOES; solid line 0.1 – 0.8 nm, dashed-dotted line 0.05 – 4 nm), (2) and (3) dm-m wave (Nançay Radiohelograph, NRH; 1D brightness distribution projected onto the solar east – west direction; axes in units of the solar radius, from $-2R_\odot$ (east) to $2R_\odot$ (west); inverse grey scale); (3) decametre-to-hectometre (DH) wave emission (*Wind*/WAVES; inverse grey scale).

1 – 14 MHz range (bottom panel) shows two faint DH type III bursts near 11:49 and 12:01 UT, but no signal during the soft X-ray burst.

The Nançay Radioheliograph (Kerdraon and Delouis, 1997) observed only long lasting emission that started well before and continued well after the flare. Time histories of the one-dimensional brightness distribution, obtained by summing 10 s integrated snapshot maps

over all pixels in the solar north – south direction, are plotted in the two central panels of Figure 1 (inverse grey scale). At dm waves (432 MHz, $\lambda = 69$ cm) a dark band, signifying bright emission, is seen at a projected distance of about 0.4 $R_{\odot}$ west of central meridian. The light grey background displays the emission of the quiet corona. The overplotted curve is the whole-Sun flux density. It shows little variation, and especially nothing peculiar during the soft X-ray burst. At metre wavelengths (164 MHz, $\lambda = 1.83$ m) numerous bursts are observed on top of a continuous emission at a similar position as at dm wavelengths. This emission is a noise storm. The two DH type III bursts are clearly related in time with two bursts of this noise storm. No dm-m-wave emission is observed from the X-class flare.

Another, but more complex, confined microwave event is plotted in Figure 2. Both the soft X-ray burst and the high-frequency microwave emission (15.4 GHz, green curve) have two components, with the microwave peaks during the rise phases of the two soft X-ray bursts. The microwave burst is visible down to a few GHz, but has no counterpart at 610 MHz (red curve) and 245 MHz (black). No DH type III burst is observed during this time either. So the microwave event is confined according to our criterion. The first emission at metre wavelengths (245 MHz, $\lambda = 1.22$ m) is a slow rise, starting after the decay of the 15.4 GHz emission, to a long-lasting plateau that extends beyond the plotted time interval. At still lower frequencies (20 – 70 MHz) a well-defined type II burst with fundamental and harmonic bands and further band splitting is observed. Shortly after its onset a short burst emanates from its low-frequency side and continues as a DH type III burst into the 1 – 14 MHz band. It shows that electrons accelerated during the metric type IV burst and the type II burst, unlike those accelerated during the impulsive phase, have access to the high corona and interplanetary space.

The third example (Figure 3) shows a non-confined microwave event with strong radio emission from microwaves to kilometric waves. It is accompanied by a major electron event seen by ACE/EPAM. The microwave emission (*cf.* 15.4 GHz; green curve) starts during the impulsive phase. It has counterparts across the dm-to-km wavelength range, as shown by the RSTN, NRH, and WAVES observations. Clearly the electrons accelerated during the impulsive phase are not confined during this event. The radio source at 164 MHz is complex, with successive brightenings in different regions. The entire phase of bright microwave-to-metre-wave emission is accompanied by an intense group of DH type III bursts.

The confined microwave event of 13 August 2004 (Figure 4) needs a more detailed discussion, because its association with enhanced particle intensities measured at L1 is ambiguous. A type III storm was observed by *Wind*/WAVES during the whole day. It was accompanied by a noise storm at metre wavelengths, whose time evolution is shown by the black curve (245 MHz) in the second panel from top in Figure 4. The event quoted as "type IV" burst in Table 1 is actually the enhancement of this noise storm appearing since about 18:15, and best seen as a succession of strong peaks near 18:40 UT, 20 – 30 min after the peak of the soft X-ray burst. It was accompanied by a hectometric – kilometric type III burst that was distinctly brighter at frequencies below 1 MHz than the others. Although the NRH observations (before 15:30 on 13 August and after 08:25 on 14 August) show that the noise storm was located above the active region where the flare occurred, the relationship of the noise storm enhancement with the X-class flare is questionable. But the acceleration process that gives rise to the noise storm enhancement is a plausible source of the particle events observed by ERNE and EPAM.

3.6. Summary of Observational Results

Using Tables 1 and 2, we summarise the observational results of this study as follows.

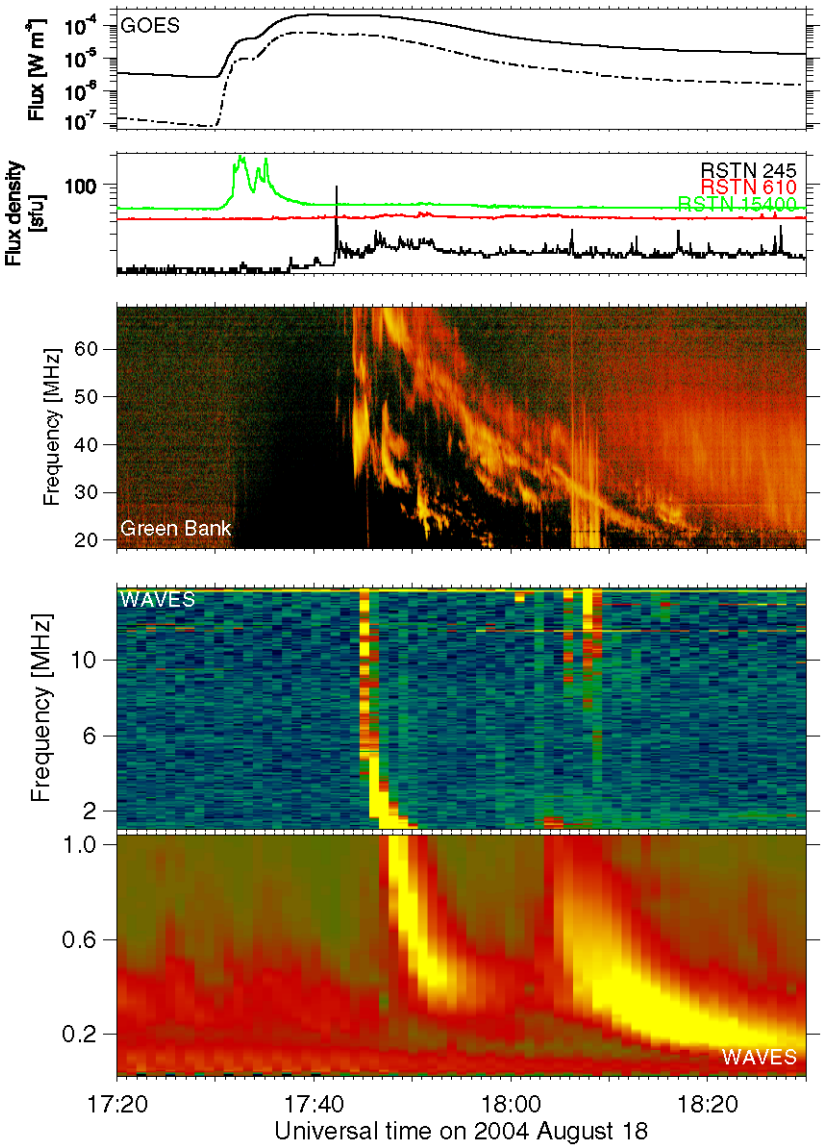

Figure 2 Time histories of X-ray and radio emissions on 18 August 2004. From top to bottom: (1) soft X-ray flux (GOES; solid line 0.1 – 0.8 nm, dashed-dotted line 0.05 – 4 nm), (2) fixed frequency flux density time profiles (RSTN Network; frequencies indicated in MHz); (3) dynamic spectrum at long metre waves (Green Bank Radio Spectrograph); (4) decametre-to-kilometre wave emission (*Wind*/WAVES). The depression of the metre wave spectrum seen during the strong soft X-ray emission is due to absorption in the Earth's atmosphere.

1. The western X-class flares that produce no SEP events at GOES are significant sources of microwave (cm-wave) emission: with respect to the statistical study of Guidice and Castelli (1975) who grouped their events into categories with peak flux densities below 50 sfu, above 500 sfu, and in between, 18/21 events are in the category of strong emitters,

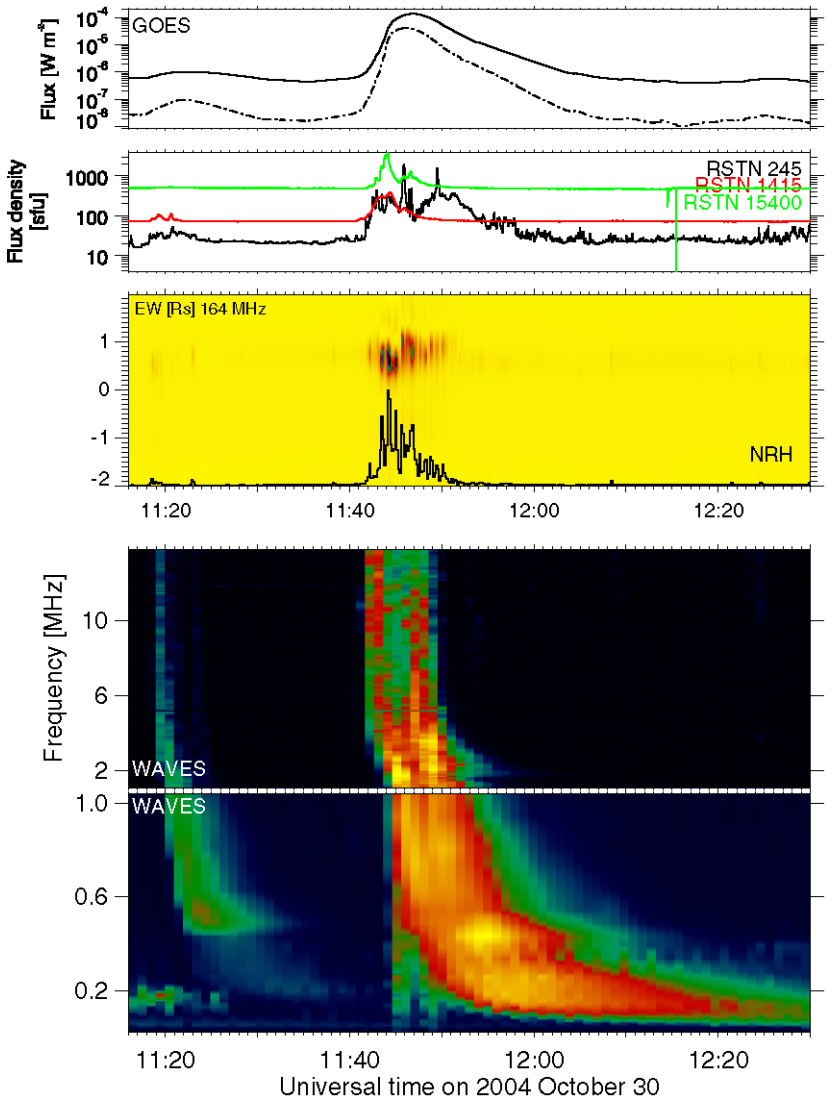

Figure 3 Time histories of X-ray and radio emissions on 30 October 2004. From top to bottom: (1) soft X-ray flux; (2) fixed frequency flux density time profiles (RSTN Network); (3) time histories of the 1D brightness distribution at m-wavelengths (inverse colour scale); (4) decametre-to-kilometre wave emission (*Wind*/WAVES).

and three in the intermediate category. While the bias towards strong events is expected, because our event sample is based on strong soft X-ray flares, this finding shows that most X-class flares without GOES SEPs are efficient electron accelerators.

2. 11/20 events where radio observations at decametric and longer wavelengths were available displayed no type III burst during the time of the most intense microwave emission, *i.e.* no evidence of electron beams escaping from the corona at that time.

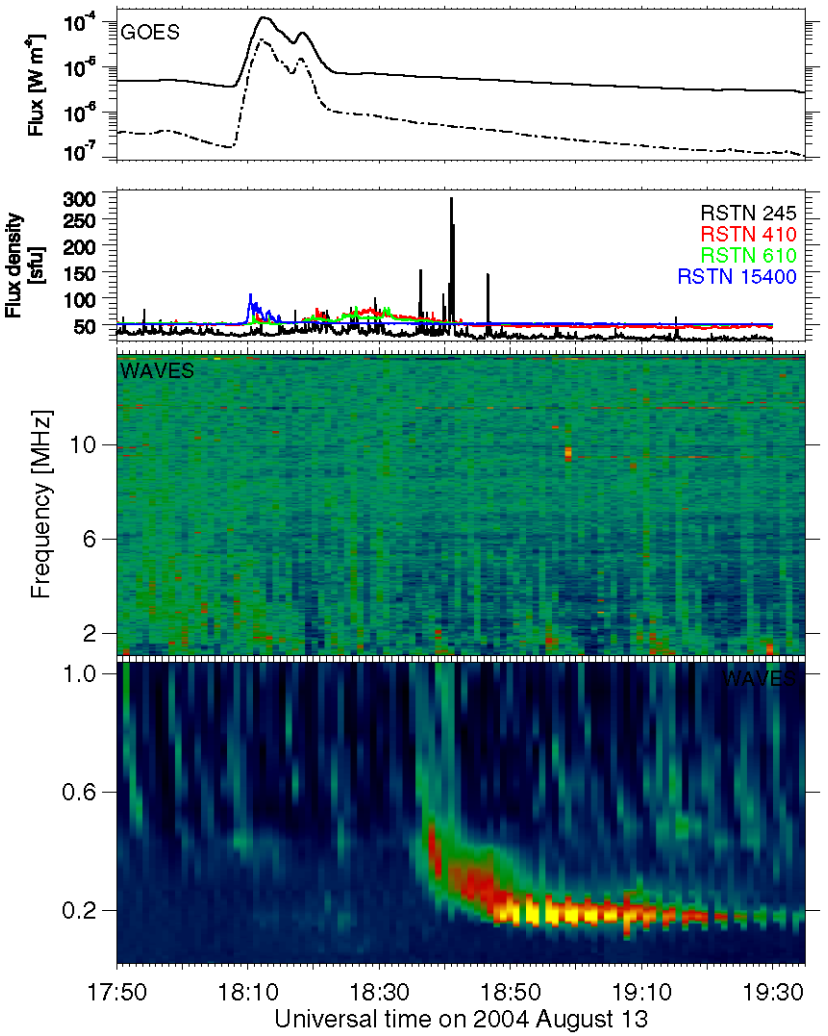

Figure 4 Time histories of X-ray and radio emissions on 13 August 2004. From top to bottom: (1) soft X-ray flux; (2) fixed frequency flux density time profiles (RSTN Network); (3), (4) decametre-to-kilometre wave emission (*Wind*/WAVES).

3. Using the presence or absence of a DH type III burst during the impulsive phase for the distinction of confined and non-confined microwave events, we find further systematic trends as follows.
   i) Peak flux density: as seen from the tables, both categories of events have comparable distributions of peak flux densities.
   ii) Peak frequency: most confined events have high peak frequency (7/11), while the numbers of low-frequency and high-frequency events are comparable in the non-confined cases.
   iii) Low frequency spectral slope: All steep low-frequency spectra are found in the confined events. Nearly half of the confined events (5/11) do have this signature. In

contrast, the non-confined microwave events have flat or intermediate low-frequency spectra.

4. The confinement of microwave emitting electrons is not equivalent with the absence of a CME. 5/11 confined microwave events are indeed CME-less. These events were already discussed in Klein, Trottet, and Klassen (2010). One further case might be CME-less, but four others are clearly accompanied by a CME. CMEs are found with all non-confined microwave events where adequate data were available.
5. Metre-wave radio emission that persists after the impulsive flare phase, especially type II bursts associated with coronal shock waves and type IV bursts associated with electron acceleration during post-eruptive reconnection in the corona, is detected in the majority of events, but more rarely with confined (5/11) than with non-confined (8 or 9/9) microwave bursts. In some events a DH type III burst during the type II or type IV emission indicates that electrons can escape to interplanetary space. This is especially the case of the confined events during which SEP are detected near L1.
6. A number of events without GOES SEPs were found to be associated with particle events detected at the L1 Lagrange point: 10/20 with electron events at tens to hundreds of keV, and 4/20 with proton events at deka-MeV energies. Electrons were detected from 4/11 confined and 6/9 non-confined microwave events, deka-MeV protons in 3/11 confined microwave events and 1/9 non-confined ones. Some uncertain cases exist, mostly because of a high background from previous events. 7/11 confined and 2/9 non-confined microwave events have no electron event detected by ACE/EPAM.

4. Discussion

4.1. Electron Confinement

A little more than half of the western X-class flares without GOES SEPs show evidence that flare-accelerated electrons are confined in magnetic structures of the low corona. The initial criterion of confinement we used, namely the absence of DH type III bursts during the impulsive phase comprising the strong microwave emission, is corroborated by other properties. A prominent one is the frequent occurrence of steep low-frequency microwave spectra that we only found during flares without a DH type III burst. Steeper spectra than predicted by gyrosynchrotron self absorption are generally ascribed to suppression of the microwave emission by the ambient medium. The plasma suppresses the transfer of energy from the energetic electrons to electromagnetic waves, an effect known as Razin suppression. This was already discussed in Klein, Trottet, and Klassen (2010) who estimated that Razin effect becomes significant at a few GHz in ambient densities of at least a few 10^{10} cm^{-3} for plausible magnetic fields of a few hundred gauss. Thermal coronal densities as high as 10^{11} cm^{-3} were reported for thick target hard X-ray emission from coronal loops by Veronig and Brown (2004), and still higher densities are required to explain the steep low-frequency microwave spectrum of the burst analysed by White *et al.* (1992). Melnikov, Gary, and Nita (2008) showed that Razin suppression may actually operate in a significant fraction of microwave bursts. We note that the event where no WAVES data were available (10 June 2003), and which was therefore excluded from the present discussion, also has a steep low-frequency spectrum, and may therefore also be a confined microwave burst.

The statistically higher peak frequency of confined microwave events is to some extent a direct consequence of the suppression of the low-frequency emission, although events with high peak frequency do not systematically display a steep low-frequency spectrum

(2/9 events with relevant data combine a high peak frequency with a steep low-frequency spectrum, while two have a high peak frequency and a flat low-frequency spectrum). In cases where the low-frequency spectrum is flat, high peak frequencies indicate strong magnetic fields. This is a further indication that the radiating electrons are confined in compact coronal structures.

It was noticed in the past that flares accelerating electrons may lack dm-m wave emission: Cliver, McNamara, and Gentile (1985) presented statistical studies of microwave bursts, and Simnett and Benz (1986), Benz *et al.* (2005) and Benz, Brajša, and Magdalenić (2007) of hard X-ray bursts. These authors showed that a fraction of 15 – 20% of the microwave or hard X-ray bursts lacked a dm-m wave counterpart. Rieger, Treumann, and Karlický (1999) discussed an intense gamma-ray flare without dm-m wave counterpart in its initial phase, and proposed that the copiously accelerated particles remained confined in low coronal structures during the impulsive phase of the flare. Trottet *et al.* (1998) showed the stepwise extension towards successively lower frequencies of the metre wave radio emission associated with another gamma-ray flare, and proposed a scenario of successive acceleration steps, during which electrons are injected into more and more extended coronal structures. Similarly, electrons accelerated during the first minutes of the large flare on 20 January 2005 remained confined in the corona (Masson *et al.*, 2009). The interpretation in terms of particle confinement during the impulsive phase provides a consistent picture with the absence of SEP events at GOES in the present study. It is in line with Kahler's finding (1982a) that a significant number of microwave bursts in the western solar hemisphere that were not followed by an SEP event lacked microwave emission below about 9 GHz.

The fact that the presence or absence of DH type III bursts reveals if particles can escape or not to space underscores the role of these bursts in SEP forecasting. Cane, Erickson, and Prestage (2002) concluded that long-lasting groups of DH type III bursts accompany most major SEP events. Laurenza *et al.* (2009) included a measure of the type III radiation at 1 MHz into their SEP forecasting scheme.

4.2. Metre-Wave Radio Emission During Confined Microwave Events

5/11 confined microwave events are accompanied by metre wave type II or type IV busts, or both. The metric radio bursts signal acceleration sites in the corona other than the region of impulsive phase acceleration. The four electron events observed during confined microwave flares all occur when these alternative accelerators exist. The acceleration of the marginal electron and proton event of 9 June 2003 at the coronal shock revealed by its type II emission was discussed by Klein, Trottet, and Klassen (2010). The three other electron events are much clearer. The related activity in the corona was a type IV burst or a noise storm enhancement. Both radio emissions are likely related to magnetic reconnection in the aftermath of a CME (Kahler and Hundhausen, 1992; Aurass, Landini, and Poletto, 2009), and CMEs were indeed observed during all three events. They had speeds up to at most 600 $\mathrm{km\,s^{-1}}$ and are therefore not expected to act primarily by their shock, although type II bursts accompanied two of them.

A detailed discussion of the relationship between different electromagnetic emissions and particles in space during the confined microwave event of 9 July 1996 was given by Laitinen *et al.* (2000). Successive electron releases could be traced back in time to discrete events of acceleration revealed in the type IV burst emission, and part of the proton acceleration, too, while another, later part, was ascribed to the interaction of the CME with the high corona and interplanetary medium. The most prominent signatures of high-energy electrons and protons in the solar atmosphere, namely microwaves, hard X-rays and nuclear gamma-rays, occurred

at a time when no type III burst was observed at lower frequencies that would have signalled the escape of particles accelerated in the impulsive flare phase. Along with the gamma-ray events cited earlier, this case illustrates particle acceleration in an evolving magnetic field, comprising a confined population in the initial phase of the flare and subsequent acceleration episodes in the higher corona, occurring as the magnetic field configuration evolves in the course of the CME.

4.3. Non-Confined Microwave Events

The detection of electron events with non-confined microwave flares, from which the flare-accelerated particles apparently have ready access to the high corona, is of course expected if the spacecraft is magnetically well connected to the flare site. Only two of the nine cases are not associated with an electron event (24 November 2000, 21 August 2002). Both were accompanied by relatively weak microwave bursts, so that these flares might be weak particle accelerators. But both had a metre wave type II burst. This confirms that the shock wave associated with the metre wave type II burst is not *a priori* an efficient particle accelerator (see Klein *et al.* (2003) and references therein). The two cases with large electron events (29 May 2003, 30 October 2004) are associated with intense microwave bursts and metre wave bursts of type II and type IV.

The effect of magnetic connection on the association of the X-class flares with SEP events is hard to assess in our data set. The only flare/CME that is well connected both in longitude and in latitude produced an electron event, despite its relatively weak microwave emission. On the other hand the poorly connected weak microwave event on 23 November 1998 also produced an electron event at ACE. The small number of cases precludes firm conclusions.

The electron events related with confined microwave flares underscore the presence of different electron (particle) accelerators in the corona. In non-confined events we are not able to distinguish the contributions of the different acceleration regions to the escaping particle populations. It may be that the combined contribution, with variable proportions, of different acceleration regions blurs the relationship between electron spectral parameters derived from the hard X-ray emission in the low solar atmosphere and from *in situ* measurements of electrons discussed by Dröge (1996) and Krucker *et al.* (2007).

4.4. Coronal Mass Ejections, Particle Acceleration and Particle Confinement

While CME-less X-class flares are confined microwave events (Gopalswamy, Akiyama, and Yashiro, 2009; Klein, Trottet, and Vilmer, 2009; Klein, Trottet, and Klassen, 2010), the present study shows that microwave events may be confined even when they are associated with a CME. Particles accelerated in the impulsive flare phase hence may remain magnetically confined while the overall magnetic structure is erupting. This is not a surprise, because the reconnection with open magnetic field lines is not necessary during the early phase of a CME, although it may occur at some later time (see, *e.g.*, the scenario of Gosling, Birn, and Hesse (1995); also Démoulin *et al.*, 2007). The confinement of flare-accelerated particles in the presence or absence of a CME suggests that the key condition for escape during the impulsive phase is the possibility to get access to pre-existing open magnetic field lines in the parent active region. This is in line with the analogous conditions for the occurrence of a CME documented by Wang and Zhang (2007) and for the occurrence of type III bursts with a given flare shown by Axisa (1974), Zlobec *et al.* (1990), and Hofmann and Ruždjak (2007): the occurrence of both a CME and a type III burst seems to be favoured when the energy release takes place in the outskirts of the parent active region.

The presence of a CME is likely the essential condition for particle acceleration to occur elsewhere in the corona, as shown by the metric type IV bursts. Type IV bursts have long been recognised as a signature of SEP-associated flares (see the historical review of Pick and Vilmer (2008) and the statistical investigation of Kahler (1982a)). They show how CMEs can play a role in SEP acceleration that is probably not related to their capacity to drive large-scale shock waves, but rather to the perturbation of the coronal magnetic field and its subsequent relaxation.

5. Conclusions: Flares, CMEs, Shocks, and the Production of SEP Events

The results of the present paper and its companion (Klein, Trottet, and Klassen, 2010) highlight the roles of flares and CMEs in the acceleration and coronal propagation of SEPs:

- Strong flares without CMEs do not produce SEP events detectable by the GOES patrol observations, mostly because the energy release occurs in a region from where the energetic particles have no access to open field lines.
- Particles accelerated in the impulsive flare phase may remain confined in the corona even when the flare is accompanied by a CME.
- CMEs themselves may create the conditions for particle acceleration in the corona after the impulsive flare phase, so that SEP events can be produced even when particles accelerated in the impulsive phase remain confined in low coronal structures.
- The effect of a CME on SEPs is not restricted to its role as the driver of a large-scale shock wave. The relaxation of magnetic stress built up in the course of a CME appears at least as relevant in the events under discussion.

These results confirm in many respects earlier work, especially by Kahler (1982a). They have been established here under cleaner observational conditions than in the past, because the confinement of particles accelerated during the impulsive flare phase allowed us to address separately acceleration scenarios related with flares and CMEs.

Acknowledgements This research was carried out partly within a collaboration between Egypt and France funded through the IMHOTEP programme. We are grateful to the coordinators of contract 18425RF, Drs. R. Helal and S. Koutchmy, and the Egyptian coordinator of contract 23190YB, Dr. M. Shaltout, for their continuous support. Our work benefited from the data of numerous space borne and ground based observatories: the ACE, SoHO and GOES spacecraft (data provided through the ACE Science Center, the ERNE data center at the University of Turku, and the National Geophysical Data Center NGDC/NOAA and the Solar Data Analysis Center at NASA/GSFC), the solar radio observatories in Athens (ARTEMIS), Berne (Inst. Applied Physics), Culgoora, Green Bank (GBSBRS), Hiraiso, Nobeyama, Potsdam (OSRA Tremsdorf), Zurich (Phoenix) and the Radio Telescope Network of the US Air Force (RSTN, data provided through NGDC), the *Wind*/WAVES experiment, as well as the Radio Monitoring web page, generated and maintained at Observatoire de Paris, Meudon, by LESIA/UMR CNRS 8109 in cooperation with the ARTEMIS team, Universities of Athens and Ioannina and the Naval Research Laboratory. Extensive use was made of the SoHO/LASCO CME catalogue, generated and maintained at the CDAW Data Center by NASA and The Catholic University of America in cooperation with the Naval Research Laboratory, and of the NEMO catalogue of coronal dimmings conceived and maintained by the Royal Observatory of Belgium. SoHO is a project of international cooperation between ESA and NASA. The authors acknowledge S. White for providing the Green Bank data of the 18 August 2004 event. They benefited from discussions at the International Space Science Institute (ISSI) in Bern, within the project "Transport of energetic particles in the inner heliosphere" led by W. Droege, and with V. Bothmer. They acknowledge constructive comments by the referee.

Appendix A: Strong Soft X-Ray Bursts and SEP Events: Observations

Table 3 gives the list of X-class flares in the western solar hemisphere and the related findings of SEP from the GOES Space Environment Monitor's Energetic Particle Sensor.[6] The columns give the date (1) and characteristic times (2) of the X-ray burst, the location inferred from Hα observations as also given in the GOES X-ray list or, if there is a difference, in *Solar Geophysical Data* (SGD) Comprehensive Reports (when put within parentheses). In some cases without flare patrol, we just indicate the quadrant where the flare was seen in SoHO/EIT daily movies.

Columns 5 – 7 give the SEP signature related to the X-ray burst. Protons of 10 MeV need about 70 min to travel a distance of 1.2 AU. When a significant rise in the GOES integral proton intensities above 10 MeV[7] was visible within a few hours after the X-ray burst, the start of the rise was evaluated, whenever possible, as the time when the exponential fit of the early rise intersects the pre-event background. If the event is in the SEP list compiled at NOAA, this is indicated in col. 7, together with the start time reported in that list. This start time differs in general from our estimate, because NOAA defines the start as the time when the intensity exceeds 10 pfu, which is most often well above the pre-event background. The difference is rarely significant, with the exception of 28 May 2003. In this case it took nearly 20 hours for the intensity to rise from background to the 10 pfu level. In col. 6 the peak integral proton intensity at energies above 10 MeV $I_{\max}$ is listed in pfu. It may be different from the NOAA list, which gives the maximum during the entire event, possibly including the Energetic Storm Particles (ESP) accelerated close to the spacecraft more than a day after the flare/CME. An ESP event usually shows up as a renewed gradual rise from the high SEP level. In this case the value of $I_{\max}$ quoted in col. 6 is the pre-ESP intensity.

A number of SEP events are actually not in the NOAA list. NOAA has two criteria to identify an event (see, *e.g.*, Balch, 2008): the integral intensity at energies above 10 MeV must exceed 10 pfu and the pre-event level must be smaller than 10 pfu. An example of a SEP event not listed by NOAA because it is too weak is 2 April 2001 10:56 UT. In some weak events it was not possible to accurately evaluate the start time. In these cases an estimated start from visual inspection is indicated. Other events were missed by NOAA because the pre-event threshold was above 10 pfu, due to a previous event. These cases are labelled 'threshold' in col. 7 (*e.g.*, 20 January 2005).

The event identification may be difficult due to enhanced flux from a previous SEP event or from an ESP event. This is then noted in cols. 5 – 7. Whenever the previous event was decaying at the time of the X-ray burst of interest, we attempted to adjust the decay by an exponential and to identify an excess above the extrapolated exponential profile that could come from the new solar event. In these cases the onset time of the start of the excess is listed (*e.g.*, 3 November 2003).

In a number of events, as on 9 July 1996, no excess above background was observed by GOES. In those cases we evaluated the background and root mean square deviation σ of the integral intensity above 10 MeV measured by GOES in an interval of 2 – 4 hours starting at the onset of the soft X-ray burst. The 3σ value is given as the upper limit of the GOES intensity in col. 6, and is complemented within parentheses by the expected value of the integral intensity above 10 MeV as defined, based on the soft X-ray properties, by Equation (6) of Garcia (2004); see also Klein, Trottet, and Klassen (2010).

[6] http://www.ngdc.noaa.gov/stp/GOES.

[7] Provided by NGDC, http://goes.ngdc.noaa.gov/data/avg/.

Table 3 GOES X-class flares and SEP signatures in the western solar hemisphere.

Date	Start, end, max (X rays; UT)	Location	Importance (Hα/X)	GOES SEP		
				Start	I_{max} [pfu]	Comment
(1)	(2)	(3)	(4)	(5)	(6)	(7)
1996 07 09	09:01 09:49 09:12	S10W30	1B/X2.6	–	< 0.19 (20)	(d)
1997 11 04	05:52 06:02 05:58	S14W33	2B/X2.1	06:35	70	NOAA 08:30 (a)
1997 11 06	11:49 12:01 11:55	S18W63	2B/X9.4	12:30	500	NOAA 13:05 (a)
1998 05 02	13:31 13:51 13:42	S15W15	3B/X1.1	13:55	150	NOAA 14:20 (a)
1998 05 06	07:58 08:20 08:09	S11W65	1N/X2.7	08:20	240	NOAA 08:45 (a)
1998 11 22	06:30 06:49 06:42	S27W82	1N/X3.7	07:45	4	(b)
1998 11 22	16:10 16:32 16:23	S30W89	2N/X2.5	≈ 16:50		decay previous (c′)
1998 11 23	06:28 06:58 06:44	S28W89	SF/X2.2	–	< 0.71 (34)	(d)
1999 08 02	21:18 21:38 21:25	S18W46	1B/X1.4	–	< 0.26 (11)	(d)
1999 08 28	17:52 18:18 18:05	S26W14	2N/X1.1	–	< 0.20 (8.7)	(d)
1999 11 27	12:05 12:16 12:12	S15W68	2B/X1.4	–	< 0.17 (9.6)	(d)
2000 03 02	08:20 08:31 08:28	(S14W52)	2B/X1.1	≈ 09:30	0.7	(b)
2000 03 22	18:34 18:56 18:48	N14W57	2N/X1.1	18:20	1	(b)
2000 03 24	07:41 07:59 07:52	N16W82	2B/X1.8	–	< 0.34 (18)	(d)
2000 06 18	01:52 02:03 01:59	N23W85	SF/X1.0	≈ 02:50	0.7	(b)
2000 07 14	10:03 10:43 10:24	N22W07	3B/X5.7	10:30	1460	NOAA 10:45 (a)
2000 11 24	04:55 05:08 05:02	(N20W05)	3B/X2.0	05:55	8	(b)
2000 11 24	14:51 15:21 15:13	N22W07	2B/X2.3	14 – 16	87	NOAA 15:20 (a)
2000 11 24	21:43 22:12 21:59	N21W14	2N/X1.8	–	< 11 (23)	decay previous (d′)
2000 11 25	18:33 18:55 18:44	N20W23	2B/X1.9			ESP event (u)
2000 11 26	16:34 16:56 16:48	N18W38	2B/X4.0	≈ 19:30		on top ESP (u)
2001 03 29	09:57 10:32 10:15	N20W19	SF/X1.7	11:50	17	NOAA 16:35 (a)
2001 04 02	10:04 10:20 10:14	N17W60	1B/X1.4	–	< 0.77 (9.8)	C (d)
2001 04 02	10:58 12:05 11:36	(N16W62)	1F/X1.1	12:30	4	(b)
2001 04 02	21:32 22:03 21:51	(NW)	EIT/X20.0	22:40	1060	NOAA 23:40 (a)
2001 04 10	05:06 05:42 05:26	S23W09	3B/X2.3	07:35	233	NOAA 08:50 (a)
2001 04 12	09:39 10:49 10:28	S19W43	SF/X2.0	≈ 11:30	50	threshold (c)
2001 04 15	13:19 13:55 13:50	S20W85	2B/X4.4	13:55	975	NOAA 14:10 (a)
2001 10 19	00:47 01:13 01:05	N16W18	2B/X1.6	01:55	7	(b)
2001 10 19	16:13 16:43 16:30	N15W29	2B/X1.6	17:40	11	NOAA 22:25 (a)
2001 10 25	14:42 15:28 15:02	S16W21	2B/X1.3	decay previous, new rise 15 – 17 UT (c′)		
2001 11 04	16:03 16:57 16:20	N06W18	3B/X1.0	16:30	3040	NOAA 17:05 (a)
2001 11 25	09:45 09:54 09:51	(SW)	EIT/X1.1	–	< 29 (6.8)	decay previous C (d′)
2002 04 21	00:43 02:38 01:51	S14W84	1F/X1.5	01:40	1980	NOAA 02:25 (a)
2002 07 03	02:08 02:16 02:13	S20W51	1B/X1.5	–	< 0.21 (10)	(d)
2002 07 15	19:59 20:14 20:08	N19W01	3B/X3.0	16/11:20	45	NOAA 16/17:50 (a)
2002 07 18	07:24 07:49 07:44	N19W30	2B/X1.8	–	< 2.6 (17)	decay previous (d′)
2002 08 03	18:59 19:11 19:07	S16W76	SF/X1.0	≈ 04/2	0.5	(b)
2002 08 21	05:28 05:36 05:34	S12W51	1B/X1.0	–	< 0.41 (4.2)	(d)
2002 08 24	00:49 01:31 01:12	S02W81	1F/X3.1	01:20	235	NOAA 01:40 (a)

Table 3 (*Continued.*)

Date	Start, end, max (X rays; UT)	Location	Importance (Hα/X)	GOES SEP Start	I_{max} [pfu]	Comment
(1)	(2)	(3)	(4)	(5)	(6)	(7)
2002 10 31	16:47 16:55 16:52	(N29W90)	/X1.2	–	< 0.74 (6.1)	C (d′)
2003 03 17	18:50 19:16 19:05	S14W39	1B/X1.5	≈ 19:45	0.8	(b)
2003 03 18	11:51 12:20 12:08	S15W46	1B/X1.5	≈ 15	0.6	(b)
2003 05 27	22:56 23:13 23:07	S07W17	2B/X1.3	cf. following event (u)		
2003 05 28	00:17 00:39 00:27	(S08W22)	1B/X3.6	04:20	≈ 10	NOAA 23:35 (a)
2003 05 29	00:51 01:12 01:05	S06W37	2B/X1.2	–	< 3.5 (7.2)	rising bg, ESP (d′)
2003 06 09	21:31 21:43 21:39	(NW)	EIT/X1.7	–	< 0.22 (12)	C (d)
2003 06 10	23:19 00:12 00:02	N10W40	2B/X1.3	–	< 0.18 (14)	(d)
2003 06 11	20:01 20:27 20:14	N14W57	1N/X1.6	–	< 0.24 (23)	(d)
2003 10 26	17:21 19:21 18:19	N02W38	1N/X1.2	17:50	294	NOAA 18:25 (a)
2003 10 29	20:37 21:01 20:49	S15W02	2B/X10.0	≈ 21:45	2530	threshold (c)
2003 11 02	17:03 17:39 17:25	S14W56	2B/X8.3	17:35	1500	threshold (c)
2003 11 03	01:09 01:45 01:30	N10W83	2B/X2.7	decay previous, new rise ≈ 3 – 4 UT (c′)		
2003 11 03	09:43 10:19 09:55	N08W77	2F/X3.9	decay previous, new rise ≈ 12 UT (c′)		
2003 11 04	19:29 20:06 19:50	S19W83	3B/X28.0	22:00	343	NOAA 22:25 (a)
2004 02 26	01:50 02:10 02:03	N14W14	SXI/X1.1	–	< 0.27 (7.4)	C (d)
2004 08 13	18:07 18:15 18:12	S13W23	SXI/X1.0	–	< 0.17 (4.7)	(d)
2004 08 18	17:29 17:54 17:40	S14W90	SXI/X1.8	–	< 0.26 (21)	(d)
2004 10 30	11:38 11:50 11:46	N13W25	SXI/X1.2	–	< 0.89 (7.3)	enhanced bg (d′)
2004 11 07	15:42 16:15 16:06	N09W17	SXI/X2.0	17:55	867	NOAA 19:10 (a)
2004 11 10	01:59 02:20 02:13	N09W49	SXI/X2.5	03:10	71	threshold (c)
2005 01 15	22:25 23:31 23:02	N15W05	SXI/X2.6	16/00:40	150	NOAA 16/02:10 (a)
2005 01 17	06:59 10:07 09:52	N15W25	SXI/X3.8	09:45	270	threshold (c)
2005 01 19	08:03 08:40 08:22	N15W51	SXI/X1.3	decay previous, new rise ≈ 08:15 (c′)		
2005 01 20	06:36 07:26 07:01	N14W61	SXI/X7.1	06:45	1700	threshold (c)
2005 07 14	10:16 11:29 10:55	N11W90	SXI/X1.2	12:55	135	threshold (c)
2005 09 15	08:30 08:46 08:38	(S11W15)	2N/X1.1	–	< 63 (4.9)	decay previous C (u)
2006 12 13	02:14 02:57 02:40	S06W23	SXI/X3.4	02:50	682	NOAA 03:10 (a)
2006 12 14	21:07 22:26 22:15	S06W46	SXI/X1.5	22:50	210	threshold (c)

Some of the soft X-ray bursts are among the 'confined' events associated with CME-less X-class bursts that were analysed in Klein, Trottet, and Klassen (2010). They are indicated by a capital 'C' in col. 7.

In summary, 69 GOES X-class flares were observed in the western solar hemisphere, *i.e.* at longitudes between 0° and 90°, between 1996 and December 2006. We distinguish five categories of events, as labelled at the end of col. 7.

i) 21 had SEP events that were catalogued by NOAA based on GOES observations.
ii) 10 had SEP events detected by GOES that were not catalogued because their peak intensity did not exceed the threshold of 10 pfu.
iii) Eight had prominent GOES SEP events that were not catalogued because the intensity at event onset was already above the threshold of 10 pfu due to a previous event. We

identified five further weak SEP events on top of previous excess intensities, and labelled them '(c′)' in col. 7.

iv) GOES/EPS showed no excess signal above background after 15 X-class flares, and six further cases where no new rise was detected on top of a high intensity from a previous event (labelled '(d′)').

v) In four cases the GOES SEP detection was uncertain because of the high background from energetic storm particles (ESP) or because of possible confusion of SEP signatures with a previous event.

Appendix B: Radio Emission and CME Association of SEP-Less X-Class Flares

Table 4 lists all western X-class flares that were not accompanied by SEP detected by GOES/EPS. The date, start and maximum time of the X-ray bursts are listed in col. 1. These times have been re-evaluated using GOES 3 s data. The start time is given as the time, rounded to the nearest minute, where the derivative of the flux starts to be persistently positive in either the 0.05 – 0.4 nm channel or the 0.1 – 0.8 nm channel, depending on which is earliest. The coincidence of this onset time with a local minimum in the flux profile has been verified by visual inspection. Properties of the microwave emission were taken from *Solar Geophysical Data* or, whenever data were available on line, derived from an analysis of the whole Sun patrol observations of the RSTN network[8] (observing frequencies: 15.4, 8.8, 4.995, 2.695, 1.415, 0.610, 0.410 and 0.245 GHz) and the Nobeyama Radio Polarimeters[9] with observing frequencies 35, 17, 9.4, 3.75, 2.0, 1.0 GHz (Nakajima *et al.*, 1985). In some events, data from the University of Bern patrol observations (courtesy A. Magun) were also used. Information on the microwave peak spectra is given in cols. 2 to 5, including the high-frequency cutoff CO(HF), the time, frequency and flux density of the spectral maximum (col. 3), in most cases the low-frequency cutoff CO(LF), and the spectral index at low frequencies (col. 5), $\alpha_{\rm lf}$. The low-frequency cutoff is only indicated when a pair of frequencies could be identified where the event is visible at the higher and invisible at the lower frequency. These two frequencies are given in col. 4. A rough characterisation of the radio emission at decimetre-to-metre wavelengths (frequency range 600 – 30 MHz) is given in col. 6, as compiled from *Solar Geophysical Data* and from observatory web sites. Column 7 indicates if a DH type III burst was observed, and if so, during which time interval, with the number of individual bursts within parentheses. This information was inferred from the *Wind*/WAVES observations at the highest observed frequency (13.8 MHz), through the evaluation of the instrument background. The indicated duration is the time interval during which the observed flux density was three standard deviations above the background level. In the 13 August 2004 event no outstanding type III burst was observed by the high-frequency detector of WAVES, but a delayed one was clearly visible at lower frequencies (≤ 1 MHz; *cf.* Figure 4). Its onset time is given, although the association with the flare is questionable because of the long delay and the low starting frequency. Column 8 contains information on the existence and timing of an associated CME. We used the catalogues of LASCO CMEs[10] and of EIT dimmings or waves.[11] The numerical values are the times when

[8] Provided by NGDC/WDC Boulder http://www.ngdc.noaa.gov/stp/SOLAR.

[9] http://solar.nro.nao.ac.jp/norp/.

[10] http://cdaw.gsfc.nasa.gov/CME_list/.

[11] http://sidc.oma.be/nemo/catalog/.

Table 4 Radio emission and CME association of western X-class flares without GOES SEP.

GOES X-ray burst	Microwaves				dm-km waves		CME/
Start, max UT	CO(HF) [GHz]	Peak	CO(LF) [GHz]	α_{lf}	dm-m-λ	DH III	dimming $t_0 - t_1$ (V, W)
(1)	(2)	(3)	(4)	(5)	(6)	(7)	(8)
1996							
Jul 09 09:04 09:11	> 15*	09:09/9 GHz/≈ 2800 sfu	–	1.3	II, IV ≥ 09:10	09:12 – 09:35 (4)	≈ 10 UT (≈450, 86°)
1998							
Nov 23 06:25 06:44	> 15*	06:35/9 GHz/≈ 700 sfu	–	1.9	III, IV (?) ≥ 06:25	06:41 – 06:48 (1)	no data
1999							
Aug 02 21:20 21:25	> 15*	21:23/≥ 15 GHz/1400 sfu	–	0.8	III, II ≥ 21:21	21:22 – 21:56 (4)	20:28 – 21:07 (292, 157°)
Aug 28 17:52 18:06	> 15*	17:59/9 GHz/≈ 2200 sfu	–	≈ 0.8	III, II ≥ 17:58	18:00 – 18:20 (4)	17:12 – 17:37 (462, 245°)
Nov 27 12:06 12:13	> 15*	12:09/15 GHz/600 sfu	–	≈ 1	III ≥ 12:15	no event	uncertain
2000							
Mar 24 07:43 07:52	> 15*	07:47/15 GHz/≈ 2000 sfu	–	1.9	DCIM, II ≥ 07:50	07:56 – 08:06 (2)	no data
Nov 24 21:43 21:59	> 15*	21:53/9 GHz/610 sfu	–	1.5	III, II ≥ 21:45	21:44 – 22:13 (4)	21:29 – 21:40 (1005, 360°)
2001							
Apr 02 10:04 10:15	> 50	10:07/15 GHz/1200 sfu	–	–	no event	storm	no CME
Nov 25 09:46 09:51	> 35	09:49/15 GHz/ ≈ 150 sfu	–	–	quiet	09:57 – 10:03 (2)	no CME
2002							
Jul 03 02:08 02:13	80 – 35	(a) 02:10/17 GHz/800 sfu	5 – 0.6	6	no event	no event	00:11 – 00:55 (265, 73°)
		(b) 02:12/17 GHz/800 sfu	1.4 – 0.6	4.9	III ≥ 02:14	02:15 – 02:37(1)	D 02:24 – 02:47
Jul 18 07:39 07:44	> 15	07:43/15 GHz/1700 sfu	–	1.2	III, IV, II ≥ 07:38	07:41 – 07:56 (1)	07:16 – 07:27 (1099, 360°)
Aug 21 05:29 05:34	> 80	05:32/17 GHz/1850 sfu	–	2.5	III, II, DCIM ≥ 05:31	05:32 – 05:37 (1)	04:05 – 04:48 (268, 66°)
Oct 31 16:48 16:53	> 15	16:51/9 GHz/3400 sfu	2.7 – 1.4	4.2	III ≥ 16:52	16:53 – 17:01 (1)	no CME

Table 4 (*Continued.*)

GOES X-ray burst	Microwaves				dm-km waves		CME/
Start, max UT	CO(HF) [GHz]	Peak	CO(LF) [GHz]	α_{lf}	dm-m-λ	DH III	dimming $t_0 - t_1$ (V, W)
(1)	(2)	(3)	(4)	(5)	(6)	(7)	(8)
2003							
May 29 00:56 01:05	> 80	01:05/9 GHz/3300 sfu	–	1.3	IV, III, II ≥ 00:58	01:02 – 01:21 (2)	00:37 – 00:46 (1237, 360°)
Jun 09 21:31 21:38	> 35	21:37/15 – 17 GHz/870 sfu	1.4 – 0.6	2.0	II F/H + prec ≥ 21:38	21:46 – 21:50 (1)	no CME
Jun 10 23:53 00:02	> 35	23:59/9 GHz/270 sfu	1.4 – 0.6	2.9	weak 245 MHz	no WAVES data	no data/ D 23:08 – 23:23
Jun 11 19:54 20:16	> 15	20:06/9 GHz/150 sfu	–	2.4	III, II ≥ 20:04	20:06 – 20:22 (1)	no data/ D 20:00 – 20:35 ?
2004							
Feb 26 01:50 02:03	> 35	01:55/9 GHz/580 sfu	3.7 – 1.0	5.8	no event	no event	no CME
Aug 13 18:07 18:12	> 15	18:10/9 GHz/570 sfu	–	4.0	dm-λ IV≥ 18:15	storm; ≈ 18:35 ≤1 MHz	18:12 – 18:40 (412, 96°)
Aug 18 17:29 17:41	> 15	17:32/> 15 GHz/1400 sfu	1.4 – 0.6	3.0	weak IV; II≥ 17:40	17:47 – 17:51 (1)	17:00 – 17:20 (602, 120,°)
Oct 30 11:36 11:47	> 15	11:44/> 15 GHz/3000 sfu	–	1.5	III, IV, II ≥ 11:41	11:44 – 12:02 (2)	11:15 – 11:42 (427, 360°)

*Based on microwave patrol reports compiled in *Solar Geophysical Data.*

the backwards extrapolated time-height trajectory of the CME front is at 0 (t_0) and 1 $R_\odot$ (t_1), respectively, with the projected speed V (in km s^{-1}) and angular width W in parentheses. In cases without LASCO observations or when the estimated CME start was different from the flare time, the detection or potential detection of a dimming listed in the NEMO catalogue is indicated by 'D' and the reported times in col. 8. The 9 July 1996 CME was only detected when it was well above the limb, and the backwards extrapolation is uncertain. Values in the table are quoted from Dryer *et al.* (1998) and Pick *et al.* (1998). A similar uncertainty occurs with the CME on 3 July 2002. The flare on 27 November 1999 occurred between several other flare/CME events in the same quadrant. The corona as seen by SoHO/LASCO is highly variable and makes new CMEs hard to identify.

References

Akimov, V.V., Ambrož, P., Belov, A.V., Berlicki, A., Chertok, I.M., Karlický, M., *et al.*: 1996, Evidence for prolonged acceleration based on a detailed analysis of the long-duration solar gamma-ray flare of June 15, 1991. *Solar Phys.* **166**, 107 – 134.

Aurass, H., Landini, F., Poletto, G.: 2009, Coronal current sheet signatures during the 17 May 2002 CME-flare. *Astron. Astrophys.* **506**, 901 – 911.

Axisa, F.: 1974, On the role of the magnetic configuration of flares for production of type III solar radio bursts. *Solar Phys.* **35**, 207 – 224.

Balch, C.C.: 2008, Updated verification of the Space Weather Prediction Center's solar energetic particle prediction model. *Space Weather* **6**, S01001.

Bastian, T.S., Benz, A.O., Gary, D.E.: 1998, Radio emission from solar flares. *Annu. Rev. Astron. Astrophys.* **36**, 131 – 188.

Belov, A., Kurt, V., Mavromichalaki, H., Gerontidou, M.: 2007, Peak-size distributions of proton fluxes and associated soft X-ray flares. *Solar Phys.* **246**, 457 – 470.

Benz, A.O., Brajša, R., Magdalenić, J.: 2007, Are there radio-quiet solar flares? *Solar Phys.* **240**, 263 – 270.

Benz, A.O., Grigis, P.C., Csillaghy, A., Saint-Hilaire, P.: 2005, Survey on solar X-ray flares and associated coherent radio emissions. *Solar Phys.* **226**, 121 – 142.

Bougeret, J.L., Kaiser, M.L., Kellogg, P.J., Manning, R., Goetz, K., Monson, S.J., *et al.*: 1995, Waves: The radio and plasma wave investigation on the *Wind* spacecraft. *Space Sci. Rev.* **71**, 231 – 263.

Brueckner, G.E., Howard, R.A., Koomen, M.J., Korendyke, C.M., Michels, D.J., Moses, J.D., *et al.*: 1995, The large angle spectroscopic coronagraph (LASCO). *Solar Phys.* **162**, 357 – 402.

Bruggmann, G., Vilmer, N., Klein, K.L., Kane, S.R.: 1994, Electron trapping in evolving coronal structures during a large gradual hard X-ray/radio burst. *Solar Phys.* **149**, 171 – 193.

Cane, H.V., Erickson, W.C., Prestage, N.P.: 2002, Solar flares, type III radio bursts, coronal mass ejections and energetic particles. *J. Geophys. Res.* **107**, 1315.

Cliver, E.W., McNamara, L.F., Gentile, L.C.: 1985, Peak flux density spectra of large solar radio bursts and proton emission from flares. *J. Geophys. Res.* **90**, 6251 – 6266.

Cliver, E.W., Dennis, B.R., Kiplinger, A.L., Kane, S.R., Neidig, D.F., Sheeley, N.R., Koomen, M.J.: 1986, Solar gradual hard X-ray bursts and associated phenomena. *Astrophys. J.* **305**, 920 – 935.

Delaboudinière, J.P., Artzner, G.E., Brunaud, J., Gabriel, A.H., Hochedez, J.F., Millier, F., *et al.*: 1995, EIT: Extreme-ultraviolet imaging telescope for the SoHO mission. *Solar Phys.* **162**, 291 – 312.

Démoulin, P., Klein, K.L., Goff, C.P., van Driel-Gesztelyi, L., Culhane, J.L., Mandrini, C.H., Matthews, S.A., Harra, L.K.: 2007, Decametric N burst: A consequence of the interaction of two coronal mass ejections. *Solar Phys.* **240**, 301 – 313.

Dröge, W.: 1996, Energetic solar electron spectra and gamma-ray observations. In: Ramaty, R., Mandzhavidze, N., Hua, X.M. (eds.) *High Energy Solar Physics*, *AIP Conf. Ser.* **374**, 78 – 85.

Dryer, M., Andrews, M.D., Aurass, H., DeForest, C., Galvin, A.B., Garcia, H., *et al.*: 1998, The solar minimum active region 7978, its X2.6/1B flare, CME, and interplanetary shock propagation of 9 July 1996. *Solar Phys.* **181**, 159 – 183.

Garcia, H.A.: 2004, Forecasting methods for occurrence and magnitude of proton storms with solar soft X-rays. *Space Weather* **2**, S02002.

Gold, R.E., Krimigis, S.M., Hawkins, S.E., Haggerty, D.K., Lohr, D.A., Fiore, E., Armstrong, T.P., Holland, G., Lanzerotti, L.J.: 1998, Electron, proton, and alpha monitor on the advanced composition explorer spacecraft. *Space Sci. Rev.* **86**, 541 – 562.

Gopalswamy, N., Akiyama, S., Yashiro, S.: 2009, Major solar flares without coronal mass ejections. In: Gopalswamy, N., Webb, D.F. (eds.) *Universal Heliophysical Processes*, *IAU Symp.* **257**, 283 – 286.
Gopalswamy, N., Yashiro, S., Krucker, S., Stenborg, G., Howard, R.A.: 2004, Intensity variation of large solar energetic particle events associated with coronal mass ejections. *J. Geophys. Res.* **109**, A12105.
Gosling, J.T., Birn, J., Hesse, M.: 1995, Three-dimensional magnetic reconnection and the magnetic topology of coronal mass ejection events. *Geophys. Res. Lett.* **22**, 869 – 872.
Guidice, D.A., Castelli, J.P.: 1975, Spectral distributions of microwave bursts. *Solar Phys.* **44**, 155 – 172.
Haggerty, D.K., Roelof, E.C.: 2002, Impulsive near-relativistic solar electron events: delayed injection with respect to solar electromagnetic emission. *Astrophys. J.* **579**, 841 – 853.
Hofmann, A., Ruždjak, V.: 2007, Favourable magnetic field configurations for generation of flare-associated meter-wave type III radio bursts. *Solar Phys.* **240**, 107 – 119.
Ippolito, A., Pommois, P., Zimbardo, G., Veltri, P.: 2005, Magnetic connection from the Earth to the solar corona, flare positions and solar energetic particle observations. *Astron. Astrophys.* **438**, 705 – 711.
Kahler, S.W.: 1982a, Radio burst characteristics of solar proton flares. *Astrophys. J.* **261**, 710 – 719.
Kahler, S.W.: 1982b, The role of the big flare syndrome in correlations of solar energetic proton fluxes and associated microwave burst parameters. *J. Geophys. Res.* **87**, 3439 – 3448.
Kahler, S.W., Hundhausen, A.J.: 1992, The magnetic topology of solar coronal structures following mass ejections. *J. Geophys. Res.* **97**, 1619 – 1631.
Kerdraon, A., Delouis, J.: 1997, The Nançay radioheliograph. In: Trottet, G. (ed.) *Coronal Physics from Radio and Space Observations*, *Lecture Notes in Physics* **483**, Springer, Berlin, 192 – 201.
Klein, K.L., Trottet, G., Vilmer, N.: 2009, A search for solar energetic particle events with CME-less flares. *Proc. 31st Int. Cosmic Ray Conf.*, Paper 0634. http://icrc2009.uni.lodz.pl/proc/pdf/icrc0634.pdf.
Klein, K.L., Trottet, G., Klassen, A.: 2010, Energetic particle acceleration and propagation in strong CME-less flares. *Solar Phys.* **263**, 185 – 208.
Klein, K.L., Schwartz, R.A., McTiernan, J.M., Trottet, G., Klassen, A., Lecacheux, A.: 2003, An upper limit of the number and energy of electrons accelerated at an extended coronal shock wave. *Astron. Astrophys.* **409**, 317 – 324.
Klein, K.L., Krucker, S., Lointier, G., Kerdraon, A.: 2008, Open magnetic flux tubes in the corona and the transport of solar energetic particles. *Astron. Astrophys.* **486**, 589 – 596.
Kocharov, L.G., Kovaltsov, G.A., Kocharov, G.E., Chuikin, E.I., Usoskin, I.G., Shea, M.A., Smart, D.F., Melnikov, V.F., Podstrigach, T.S., Armstrong, T.P.: 1994, Electromagnetic and corpuscular emission from the solar flare of 1991 June 15: continuous acceleration of relativistic particles. *Solar Phys.* **150**, 267 – 283.
Krucker, S., Kontar, E.P., Christe, S., Lin, R.P.: 2007, Solar flare electron spectra at the Sun and near the Earth. *Astrophys. J. Lett.* **663**, 109 – 112.
Laitinen, T., Klein, K.L., Kocharov, L., Torsti, J., Trottet, G., Bothmer, V., Kaiser, M.L., Rank, G., Reiner, M.J.: 2000, Solar energetic particle event and radio bursts associated with the 1996 July 9 flare and coronal mass ejection. *Astron. Astrophys.* **360**, 729 – 741.
Laurenza, M., Cliver, E.W., Hewitt, J., Storini, M., Ling, A.G., Balch, C.C., Kaiser, M.L.: 2009, A technique for short-term warning of solar energetic particle events based on flare location, flare size, and evidence of particle escape. *Space Weather* **7**, S04008.
Marqué, C., Posner, A., Klein, K.L.: 2006, Solar energetic particles and radio-silent fast coronal mass ejections. *Astrophys. J.* **642**, 1222 – 1235.
Masson, S., Klein, K.L., Bütikofer, R., Flückiger, E.O., Kurt, V., Yushkov, B., Krucker, S.: 2009, Acceleration of relativistic protons during the 20 January 2005 flare and CME. *Solar Phys.* **257**, 305 – 322.
Melnikov, V.F., Gary, D.E., Nita, G.M.: 2008, Peak frequency dynamics in solar microwave bursts. *Solar Phys.* **253**, 43 – 73.
Nakajima, H., Sekiguchi, H., Sawa, M., Kai, K., Kawashima, S.: 1985, The radiometer and polarimeters at 80, 35, and 17 GHz for solar observations at Nobeyama. *Publ. Astron. Soc. Japan* **37**, 163 – 170.
Nindos, A., Aurass, H., Klein, K.L., Trottet, G.: 2008, Radio emission of flares and coronal mass ejections. *Solar Phys.* **253**, 3 – 41.
Nita, G.M., Gary, D.E., Lee, J.: 2004, Statistical study of two years of solar flare radio spectra obtained with the Owens Valley Solar Array. *Astrophys. J.* **605**, 528 – 545.
Nolte, J.T., Roelof, E.C.: 1973, Large-scale structure of the interplanetary medium, I: high coronal source longitude of the quiet-time solar wind. *Solar Phys.* **33**, 241.
Pick, M.: 1986, Observations of radio continua and terminology. *Solar Phys.* **104**, 19 – 32.
Pick, M., Vilmer, N.: 2008, Sixty-five years of solar radioastronomy: flares, coronal mass ejections and Sun Earth connection. *Astron. Astrophys. Rev.* **16**, 1 – 153.
Pick, M., Maia, D., Kerdraon, A., Howard, R., Brueckner, G.E., Michels, D.J., *et al.*: 1998, Joint Nancay Radioheliograph and LASCO observations of coronal mass ejections – II. The 9 July 1996 event. *Solar Phys.* **181**, 455 – 468.

Rieger, E., Treumann, R.A., Karlický, M.: 1999, The radio-silent start of an intense solar gamma-ray flare. *Solar Phys.* **187**, 59 – 75.

Simnett, G.M., Benz, A.O.: 1986, The role of metric and decimetric radio emission in the understanding of solar flares. *Astron. Astrophys.* **165**, 227 – 234.

Torsti, J., Valtonen, E., Lumme, M., Peltonen, P., Eronen, T., Louhola, M., *et al.*: 1995, Energetic particle experiment ERNE. *Solar Phys.* **162**, 505 – 531.

Trottet, G.: 1986, Relative timing of hard X-rays and radio emissions during the different phases of solar flares – consequences for the electron acceleration. *Solar Phys.* **104**, 145 – 163.

Trottet, G., Vilmer, N., Barat, C., Benz, A., Magun, A., Kuznetsov, A., Sunyaev, R., Terekhov, O.: 1998, A multiwavelength analysis of an electron-dominated gamma-ray event associated with a disk solar flare. *Astron. Astrophys.* **334**, 1099 – 1111.

Veronig, A.M., Brown, J.C.: 2004, A coronal thick-target interpretation of two hard X-ray loop events. *Astrophys. J. Lett.* **603**, 117 – 120.

Wang, Y., Zhang, J.: 2007, A comparative study between eruptive X-class flares associated with coronal mass ejections and confined X-class flares. *Astrophys. J.* **665**, 1428 – 1438.

White, S.M., Kundu, M.R., Bastian, T.S., Gary, D.E., Hurford, G.J., Kucera, T., Bieging, J.H.: 1992, Multi-frequency observations of a remarkable solar radio burst. *Astrophys. J.* **384**, 656 – 664.

Zlobec, P., Messerotti, M., Ruzdjak, V., Vrsnak, B., Karlicky, M.: 1990, The role of the magnetic field intensity and geometry in the type III burst generation. *Solar Phys.* **130**, 31 – 37.